Nonfullerene Polymer Solar Cells based on a Perylene Monoimide Acceptor with a High Open-Circuit Voltage of 1.3 V

Youdi Zhang, Xia Guo, Bing Guo, Wenyan Su, Maojie Zhang,* and Yongfang Li**

Nonfullerene polymer solar cells (PSCs) are fabricated with a perylene monoimide-based n-type wide-bandgap organic semiconductor PMI-F-PMI as an acceptor and a bithienyl-benzodithiophene-based wide-bandgap copolymer PTZ1 as a donor. The PSCs based on PTZ1:PMI-F-PMI (2:1, w/w) with the treatment of a mixed solvent additive of 0.5% *N*-methyl pyrrolidone and 0.5% diphenyl ether demonstrate a very high open-circuit voltage (V_{oc}) of 1.3 V with a higher power conversion efficiency (PCE) of 6%. The high V_{oc} of the PSCs is a result of the high-lying lowest unoccupied molecular orbital (LUMO) of −3.42 eV of the PMI-F-PMI acceptor and the low-lying highest occupied molecular orbital (HOMO) of −5.31 eV of the polymer donor. Very interestingly, the exciton dissociation efficiency in the active layer is quite high, even though the LUMO and HOMO energy differences between the donor and acceptor materials are as small as ≈0.08 and 0.19 eV, respectively. The PCE of 6% is the highest for the PSCs with a V_{oc} as high as 1.3 V. The results indicate that the active layer based on PTZ1/PMI-F-PMI can be used as the front layer in tandem PSCs for achieving high V_{oc} over 2 V.

1. Introduction

The bulk heterojunction polymer solar cells (PSCs) based on conjugated polymers as donor and fullerene derivatives as acceptor have attracted much interest due to their advantages of light weight, flexibility, and low-cost solution processing.[1–5] The key factors that determine the power conversion efficiency (PCE) of the PSCs are the open-circuit voltage (V_{oc}), short-circuit current density (J_{sc}), and fill factor (FF). V_{oc} is directly proportional to the offset between the lowest unoccupied molecular orbital (LUMO) level of the acceptor and the highest occupied molecular orbital (HOMO) level of the donor.[6] Hence, V_{oc} of the PSCs can be effectively improved by elevating the LUMO level of the acceptor or/and decreasing the HOMO level of the donor.[7–25]

In the past few years, plenty of works successfully improved V_{oc} of PSCs by decreasing HOMO levels of conjugated polymer donors through modulating the backbones[23,26–29] or tuning side chains.[20,24,30–33] However, the V_{oc} of PSCs based on commonly used fullerene derivative PCBM acceptor is difficult to exceed 1.0 V, limited by its lower LUMO level. Therefore, upshifting the LUMO level of acceptors is needed to increase V_{oc}.[8,34] For example, indene-C_{70}-bisadduct ($IC_{70}BA$) synthesized by He et al.[8] exhibited a higher LUMO of −3.71 eV compared with that of [6,6]-phenyl-C_{61}-butyric acid methyl ester ($PC_{61}BM$) or [6,6]-phenyl-C_{71}-butyric acid methyl ester ($PC_{71}BM$) (−3.90 eV), then the PSCs based on poly(3-hexylthiophene) (P3HT):$IC_{70}BA$ show the improved PCE of ≈7.4% with increased V_{oc} of 0.87 V compared to the PSCs based on P3HT:$PC_{71}BM$ (PCE of ≈4.4% and V_{oc} of 0.61 V).[9] Recently, PSCs based on n-type organic semiconductor (n-OS) as acceptor have exhibited high V_{oc}, due to the higher-lying LUMO of the n-OS. For instance, an n-OS SF(DPPB)$_4$ based on a spirobifluorene core with four diketopyrrolopyrrole (DPP) arms possesses a higher-lying LUMO level of −3.51 eV and the nonfullerene PSCs based on P3HT as donor and SF(DPPB)$_4$ as acceptor demonstrated a maximum PCE of 5.1% with a high V_{oc} of 1.1 V.[35] Recently, Geng and Xie and co-workers synthesized a D–A structured oligomer containing benzothiadiazole and fluorene units, F4TBT4, with a LUMO of −3.2 eV, and a high V_{oc} of 1.2 V was achieved for the PSCs based on P3HT/F4TBT4 with a PCE of 4.12%.[36] Yu et al. fabricated all polymer solar cells with a conjugated polymer PFTBT-OC_6 as acceptor and P3HT as donor, which showed a V_{oc} as high as 1.3 V but a low PCE of 1.8%.[37] Bo et al. synthesized a series of 1,8-naphthalimide (NI)-based n-OS acceptors which demonstrated high V_{oc} of over 1.0 V with PCE of 2.0%–4.0% in the corresponding nonfullerene PSCs.[38–41] Yan and co-workers recently reported a high-performance n-OS acceptor of perylene diimide (PDI)

Dr. Y. Zhang, Dr. X. Guo, B. Guo, W. Su,
Prof. M. Zhang, Prof. Y. Li
State and Local Joint Engineering Laboratory for Novel Functional Polymeric Materials
Laboratory of Advanced Optoelectronic Materials
College of Chemistry, Chemical Engineering and Materials Science
Soochow University
Suzhou 215123, China
E-mail: guoxia@suda.edu.cn; mjzhang@suda.edu.cn; liyf@iccas.ac.cn
Y. Li
Beijing National Laboratory for Molecular Sciences
CAS Key Laboratory of Organic Solids
Institute of Chemistry
Chinese Academy of Sciences
Beijing 100190, China

DOI: 10.1002/adfm.201603892

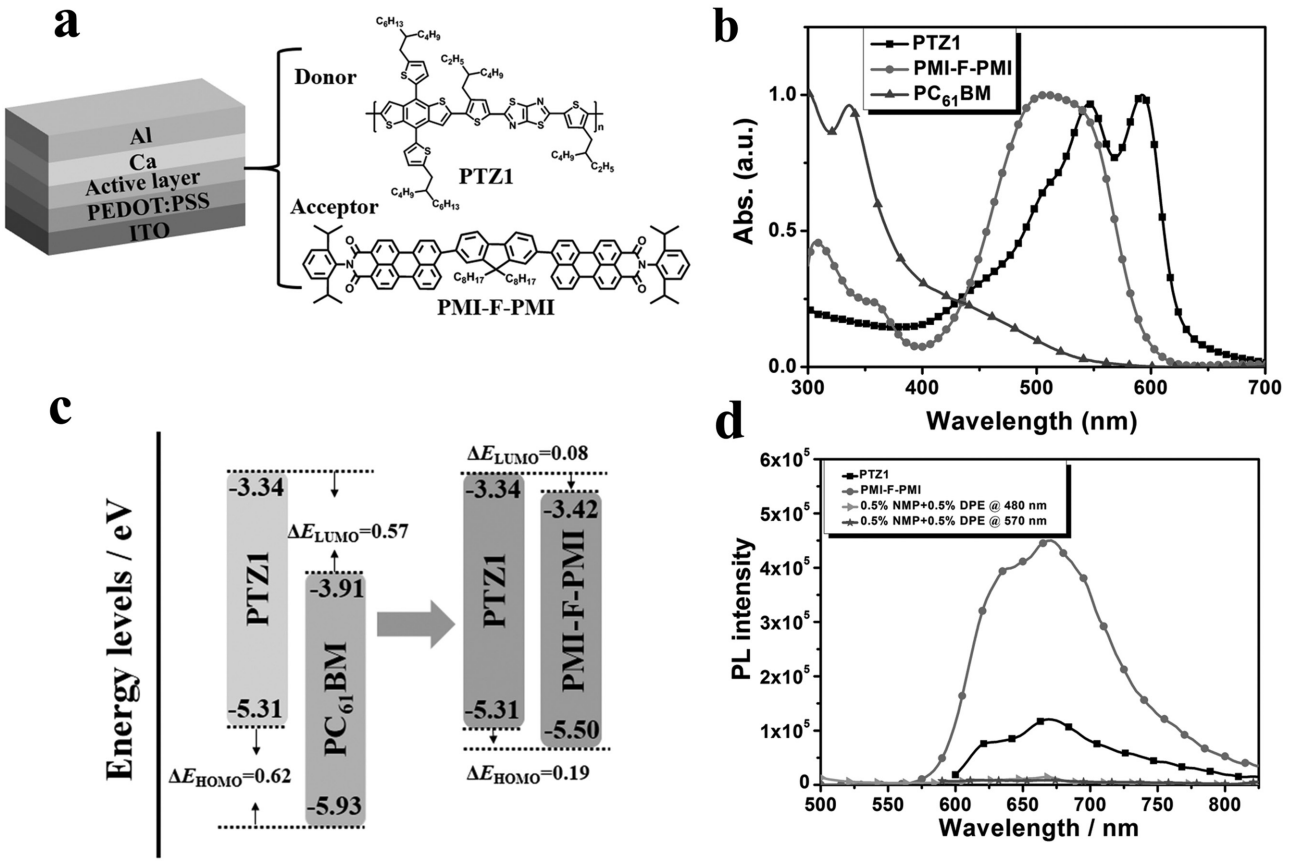

Figure 1. a) Device architecture and chemical structures of the donor and the acceptor materials. b) Normalized absorption spectra of PTZ1, PMI-F-PMI, and $PC_{61}BM$ films prepared from chloroform solutions. c) Electronic energy levels of PTZ1, PMI-F-PMI, and $PC_{61}BM$. d) Photoluminescence spectra of the films of PMI-F-PMI, PTZ1, and PTZ1:PMI-F-PMI (2:1, w/w) with the mixed solvent additive (0.5% NMP and 0.5% DPE) treatment.

derivative (SF-PDI2), and the nonfullerene PSC with a difluorobenzothiadiazole-based D–A copolymer (PffBT4T-2DT) as donor and SF-PDI2 as acceptor showed a high V_{oc} of 0.98 V with a PCE of 6.3%.[42]

Here, we fabricated a nonfullerene polymer solar cell with a wide-bandgap polymer PTZ1 (see **Figure 1**a) as donor and a perylene monoimide (PMI)-based n-OS PMI-F-PMI as acceptor for achieving high V_{oc} PSCs with high PCE. PTZ1 exhibited a deep HOMO energy level of −5.31 eV, a relatively high hole mobility of 3.86×10^{-3} cm^2 V^{-1} s^{-1}, a face-on predominated molecular orientation, and a higher PCE of 7.7% and a high V_{oc} of 0.94 V in the $PC_{71}BM$-based PSCs,[43] while PMI-F-PMI possesses a higher-lying LUMO level of −3.42 eV.[44] The nonfullerene PSCs based on PTZ1/PMI-F-PMI (2:1, w/w) demonstrated an optimum PCE of 6.0% with a high V_{oc} of 1.30 V, a J_{sc} of 7.2 mA cm^{-2}, and an impressive FF of 63.5%. The PCE of 6.0% is the highest efficiency for the PSCs with V_{oc} as high as 1.3 V. Moreover, both the donor and acceptor are wide-bandgap materials, so the active layer of PTZ1/PMI-F-PMI could be used as a front layer in tandem PSCs for achieving high V_{oc} over 2 V, which will be beneficial for the potential application in water splitting by photocatalysis.[45–47]

2. Results and Discussion

2.1. Absorption Spectra and Energy Levels

Figure 1a shows the device structure of the PSCs based on PTZ1:PMI-F-PMI and the molecular structures of the donor and acceptor materials. We also fabricated the PSCs based on PTZ1:$PC_{61}BM$ as control device. And different solvent additives of *N*-methyl pyrrolidone (NMP) and diphenyl ether (DPE) were used to optimize photovoltaic performance of the devices. Figure 1b displays the absorption spectra of the polymer donor PTZ1 and the acceptors of PMI-F-PMI and $PC_{61}BM$. It can be seen that the absorption of PMI-F-PMI film is much broader than that of $PC_{61}BM$ in the visible range, and is partially complementary with that of PTZ1 film.

Figure 1c shows electronic energy levels of the donor and acceptor materials, which were measured by electrochemical cyclic voltammetry as shown in Figure S1 in the Supporting Information. The LUMO and HOMO energy levels of PMI-F-PMI acceptor are −3.42 and −5.50 eV, respectively. Obviously, −3.42 eV is a relatively higher LUMO level for the acceptors in PSCs. In order to more deeply understand the higher-lying LUMO energy level of PMI-F-PMI, we performed theoretical

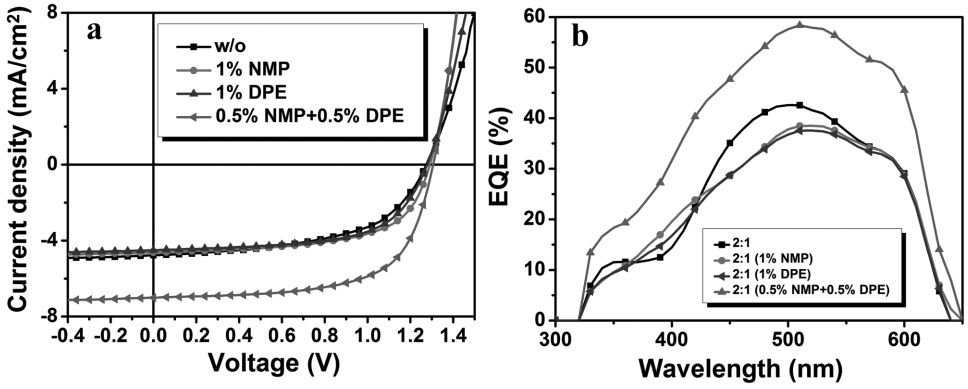

Figure 2. a) *J–V* curves and b) EQE curves of the PSCs based on PTZ1:PMI-F-PMI (2:1, w/w) under the illumination of AM 1.5G, 100 mW cm^{-2}.

calculations on the HOMO and LUMO energy levels and electron density distribution of PMI-F-PMI and the monomers PDI and PMI (for comparison) by density functional theory at the B3LYP/6-31G level (Figure S2, Supporting Information). The calculated LUMO and HOMO levels are −2.90 and −5.46 eV for PMI-F-PMI, −2.82 and −5.55 eV for PMI, and −3.49 and −6.01 eV for PDI, respectively. The LUMO level of PMI is significantly upshifted than that of PDI, and it is reasonable for PMI-F-PMI with the LUMO level downshifted and HOMO level upshifted than those of PMI monomer.

The large energy difference of 1.89 eV between the LUMO (−3.42 eV) of PMI-F-PMI acceptor and the HOMO (−5.31 eV) of the PTZ1 donor will benefit to a high V_{oc} of the nonfullerene PSCs. However, the LUMO energy difference (ΔE_{LUMO}) (0.08 eV) and HOMO energy difference (ΔE_{HOMO}) (0.19 eV) between PTZ1 donor and PMI-F-PMI acceptor seems too low for the excitons dissociation to overcome the binding energy of the excitons. To investigate if the exciton dissociation and charge transfer can effectively occur in the active layers of the PSCs with such low ΔE_{LUMO} and ΔE_{HOMO}, we measured photoluminescence (PL) quenching behavior of the PTZ1:PMI-F-PMI blend films with the treatment of a mixed solvent additive of 0.5% NMP and 0.5% DPE. (The mixed solvent treatment is an optimized condition for achieving high photovoltaic performance of the PSCs, which will be discussed below.) Figure 1d and Figure S3 in the Supporting Information show the PL spectra of the pure donor, pure acceptor, and the blend films treated with the mixed solvent additive. It can be seen that over 90% and 99% PL quenching of PMI-F-PMI acceptor and PTZ1 donor, respectively, were observed for the PMI-F-PMI:PTZ1 blend films with the treatment of the mixed solvent additives, in comparison with the PL spectra of the pure donor and pure acceptor. The PL quenching efficiency was obtained by calculating the ratio of the integrate area of PL peak between the blend film and pure film (polymer donor or n-OS acceptor). The results indicate that efficient exciton dissociation and charge transfer occur between PTZ1 and PMI-F-PMI, even though the ΔE_{LUMO} and ΔE_{HOMO} are small for the PTZ1: PMI-F-PMI blend films.

2.2. Photovoltaic Properties

The nonfullerene PSCs based on PTZ1:PMI-F-PMI were fabricated with the conventional device structure of ITO/PEDOT:PSS/PTZ1:PMI-F-PMI/Ca/Al. And the control PSCs based on PTZ1:$PC_{61}BM$ were also fabricated with the similar conventional device structure. The photovoltaic properties of the PTZ1:PMI-F-PMI-based PSCs were optimized by changing different D/A weight ratios and by using a trace amount of NMP and DPE solvent additive. **Figure 2**a shows the current density–voltage (*J–V*) curves of the PSCs based on PTZ1:PMI-F-PMI (2:1, w/w) under the illumination of AM 1.5G, 100 mW cm^{-2}. The photovoltaic parameters, including the short-circuit current density (J_{sc}), the open-circuit voltage (V_{oc}), FF, and PCE, were outlined in **Table 1**. First, we investigated the effect of D/A weight ratios (3:1, 2:1, and 1:1) of PTZ1:PMI-F-PMI blend on the photovoltaic performance of the PSCs. Obviously, the optimal D/A weight ratio is 2:1 (Table 1), and the optimum PCE of the PTZ1:PMI-F-PMI-based device reached 3.3% with a V_{oc} of 1.3 V, a J_{sc} of 4.8 mA cm^{-2}, and FF of 54.2%. Then, with the optimum D/A weight ratio of 2:1, different solvent additives (NMP and DPE) were used to further optimize the photovoltaic performance, and the results are shown in Figure S3 and Table S1 in the Supporting Information. The PCE of the PSCs was slightly improved to 3.6%, with a V_{oc} of 1.3 V, a J_{sc} of 4.6 mA cm^{-2}, and FF of 60.9% by using

Table 1. Photovoltaic properties of the PSCs based on PTZ1:PMI-F-PMI with different D/A ratios and additives treatment under the illumination of AM 1.5G, 100 mW cm^{-2}.

D/A [w/w]	Additives	V_{oc} [V]	J_{sc} [mA cm^{-2}]	FF [%]	PCE_{max}/PCE_{ave}[a)] [%]/[%]	Thickness [nm]
3:1	w/o	1.32 ± 0.02	3.7 ± 0.1	56.2 ± 1.2	2.9/2.8	85
2:1	w/o	1.27 ± 0.01	4.6 ± 0.2	55.2 ± 0.9	3.3/3.2	95
2:1	1% NMP	1.29 ± 0.01	4.5 ± 0.1	60.0 ± 0.8	3.6/3.5	80
2:1	1% DPE	1.28 ± 0.01	4.4 ± 0.2	60.2 ± 0.9	3.5/3.4	84
2:1	0.5% NMP + 0.5% DPE	1.30 ± 0.01	7.0 ± 0.2	63.5 ± 0.4	6.0/5.7	93
1:1	w/o	1.30 ± 0.02	3.1 ± 0.1	49.0 ± 0.8	2.1/2.0	90
1:1.25[b)]	1% DIO[c)]	0.87 ± 0.02	7.1 ± 0.2	61.2 ± 0.5	4.0/3.8	80

[a)]Average values are obtained from ten devices; [b)]PTZ1:$PC_{61}BM$ as control device is tested; [c)]DIO as a solvent additive is 1, 8-diiodooctane.

1 vol% NMP additive treatment. While DPE solvent additive treatment did not show obvious improvement on the efficiency (Figure S4, Supporting Information). Interestingly, PCE of the PSCs was greatly improved to 6.0% with a high V_{oc} of 1.30 V, a J_{sc} of 7.2 mA cm^{-2}, and a high FF of 63.5% by using 0.5% NMP and 0.5% DPE mixed additives treatment. For the control device based on PTZ1:$PC_{61}BM$, the best PCE was 4.0% with a V_{oc} of 0.9 V, a J_{sc} of 7.3 mA cm^{-2}, and an FF of 61.8% (Table 1). Obviously, the V_{oc} of the PTZ1:PMI-F-PMI-based PSCs is much higher than that of the control device with $PC_{61}BM$ as acceptor. The high V_{oc} of the PSCs should be a result of the high-lying LUMO of the PMI-F-PMI acceptor. For the J_{sc} of 7.3 mA cm^{-2}, although it is not a high value for PSCs at present, it is a good value for the device based on PTZ1:PMI-F-PMI with the small ΔE_{LUMO} and ΔE_{HOMO} values between the polymer donor and the n-OS acceptor. Probably, the driving force may not be the most important factor influencing the charge separation kinetics for the PTZ1:PMI-F-PMI blends as that of the P3TEA:SF-PDI_2 blend reported recently by Yan and co-workers[48] and Wang et al.[49]

Figure 2b shows the external quantum efficiency (EQE) curves of the PSCs based on PTZ1:PMI-F-PMI (2:1, w/w) without and with additives. The maximum EQE value was corresponding to the absorption of acceptor material PMI-F-PMI at ≈510 nm. The higher EQE values corresponding to the acceptor absorption are reasonable because of the larger HOMO energy difference between the donor and acceptor photovoltaic materials. The current density obtained by the integration of the EQE curves with the standard AM 1.5G solar spectrum is consistent with the J_{sc} values from the J–V curves within 5% error, which indicates that the photovoltaic parameters are reliable. By comparing EQE value of PTZ1:PMI-F-PMI-based device (2:1, w/w) without and with 1% NMP additives, the maximum EQE value in the visible light region of ≈400–640 nm was decreased from 43% to 39%, which was consistent with the dropped J_{sc} of the devices with the 1% NMP additive treatment. Then, when the mixed additives (0.5% NMP and 0.5% DPE) were used in the treatment, the maximum EQE value was enhanced to 58% at 510 nm, which agrees well with the higher J_{sc} for the devices with the mixed solvent additive treatment.

It should be mentioned that Holliday et al. synthesized an n-OS (5Z,5Z′)-5,5′-((7,7′-(9,9-dioctyl-9H-fluorene-2,7-diyl) bis(benzo[c]1,2,5]thiadiazole-7,4-diyl))bis(methanylylidene)) bis(3-ethyl-2-thioxothiazolidin-4-one) (FBR) with fluorene as a core unit, and the nonfullerene PSCs with FBR as an acceptor and P3HT as a donor achieved a PCE of 4.1%.[50] Subsequently, they improved the photovoltaic performance of the n-OS acceptor by replacing fluorene core with a larger fused ring indacenodithiophene (IDT) unit (the PCE of the nonfullerene PSCs reached 6.4%).[51] Probably, if we replace the fluorine core of PMI-F-PMI with IDT unit, the photovoltaic performance could be further increased. The related synthesis is under way in our laboratory.

2.3. Hole and Electron Mobilities

In order to better understand the effect of solvent additives treatment on the photovoltaic performance of the PSCs based on PTZ1:PMI-F-PMI, we implemented characterization of the charge carrier mobilities by using the space-charge-limited current (SCLC) method[52] for PTZ1:PMI-F-PMI blend without and with the solvent additive treatment of 1% NMP, 1% DPE, and mixed additives (0.5% NMP and 0.5% DPE). The current–voltage plots for the mobility measurements were shown in Figure S5 in the Supporting Information, and the electron (μ_e) and hole (μ_h) mobility values were summarized in **Table 2**. The electron mobility of PMI-F-PMI was measured to be 1.0×10^{-3} cm^2 V^{-1} s^{-1}, which was in identical order of magnitude as that of $PC_{61}BM$ (Figure S6 and Table S2, Supporting Information).[53] It is important to note that μ_e of PTZ1:PMI-F-PMI blend with additives was superior to that of device without additive, and μ_h values were obviously higher than μ_e values in all devices, indicating μ_e played an important role in the limitation of photovoltaic performance, in particular for J_{sc}. The μ_e (2.02×10^{-4} cm^2 V^{-1} s^{-1}) of the blend based on PTZ1:PMI-F-PMI (w/w 2:1) with 1% NMP was close to that (1.23×10^{-4} cm^2 V^{-1} s^{-1}) with 1% DPE. The results of electron mobilities were consistent with the photovoltaic properties of the devices based on PTZ1:PMI-F-PMI with 1% NMP and 1% DPE additive treatments. By using mixed solvent additives of 0.5% NMP and 0.5% DPE, the PTZ1:PMI-F-PMI-based device showed the highest electron mobility value of 4.93×10^{-4} cm^2 V^{-1} s^{-1}, while the μ_h (3.35×10^{-3} cm^2 V^{-1} s^{-1}) was lower than that of the device without additive (5.12×10^{-3} cm^2 V^{-1} s^{-1}), and was similar to that of the device with 1% NMP or 1% DPE additive treatments (3.26×10^{-3} and 3.23×10^{-3} cm^2 V^{-1} s^{-1}, respectively). The relatively higher and more balanced hole and electron mobilities are obtained in the blend film treated by the mixed solvent additives, which are beneficial to the reduction of recombination and the improvement of the photovoltaic performance of the devices. The results indicate that a favorable D/A bicontinuous network could be formed to facilitate charge transport in the blend film with the mixed additives treatment.[54]

Table 2. Hole and electron mobility values of the PTZ1:PMI-F-PMI blends without and with different additives treatment, measured by the SCLC method.

Additives	μ_e [cm^2 V^{-1} s^{-1}]	μ_h [cm^2 V^{-1} s^{-1}]
w/o	8.22×10^{-5}	5.12×10^{-3}
1% NMP	2.02×10^{-4}	3.26×10^{-3}
1% DPE	1.23×10^{-4}	3.23×10^{-3}
0.5% NMP + 0.5% DPE	4.93×10^{-4}	3.35×10^{-3}

2.4. Studies on the Charge Carriers Recombination of the PSCs

To better understand the charge recombination processes of the PSCs based on PTZ1:PMI-F-PMI blends, light-intensity-dependent J_{sc} and V_{oc} characteristics were performed.[55] Exciton generation rates and the charge collection probabilities (P_C, determined by the normalized J_{ph} at the saturated current density) were revealed by using plots of the photocurrent density (J_{ph}) versus effective voltage (V_{eff}) at J_{sc} conditions, as

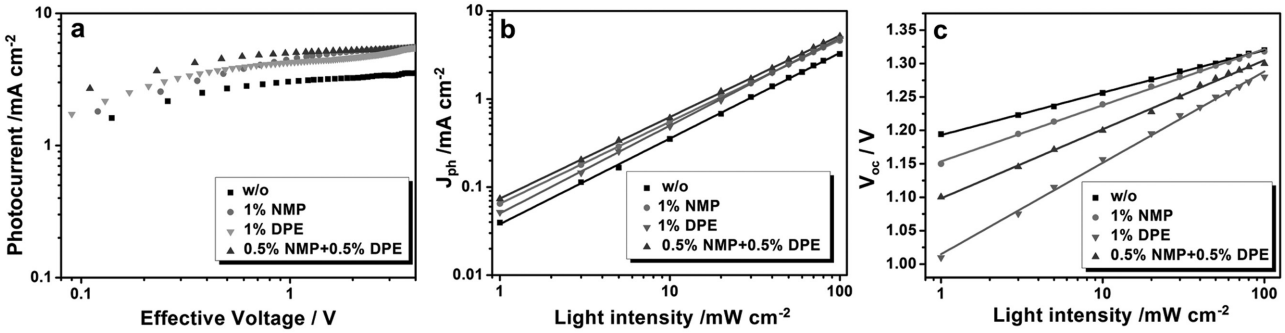

Figure 3. a) J_{ph}–V_{eff}, b) J_{sc}–P, and c) V_{oc}–P curves of the devices based on PTZ1:PMI-F-PMI. The solid lines are the fitted lines in the J_{sc}–P and V_{oc}–P plots.

shown in **Figure 3**a. J_{ph} has been defined by $J_{ph} = J_L - J_D$, where J_L and J_D are the current densities under illumination of AM 1.5G, 100 mW cm^{-2} and in the dark condition respectively. And $V_{eff} = V_0 - V_{appl}$, where V_0 is the voltage at which $J_{ph} = 0$, and V_{appl} is the applied bias voltage. The saturated photocurrent was observed at $V_{eff} = 2$–4 V and the resulting P_C was determined to be 90%, 93%, 92%, and 98% for PTZ1:PMI-F-PMI blend film without and with the treatments of 1% NMP, 1% DPE, and mixed additives (0.5% NMP and 0.5% DPE) under short-circuit conditions, respectively. The higher P_C value of 98% for the PTZ1:PMI-F-PMI blend with the mixed additives treatment is consistent with the superior photovoltaic performance of the device in comparison with the devices without and with 1% NMP and 1% DPE solvent additives.

The light intensity (P) dependences of J_{sc} and V_{oc} were also measured to investigate nongeminate recombination losses of the devices. The relationship between J_{sc} and light intensity followed the relation $J_{sc} \propto P^S$.[56] The S values were calculated to be 0.93, 0.95, 0.94, and 0.98, respectively, from the J_{sc}–P curves in Figure 3b for PTZ1:PMI-F-PMI blend film without and with the treatments of 1% NMP, 1% DPE, and mixed additives respectively. The S value of 0.98 (near to 1.00) for the device with the mixed solvent additive treatment signified that the bimolecular recombination was negligible in the device, which is superior to other devices without or with a single solvent additive treatment. The V_{oc}–P curves were shown in Figure 3c, the V_{oc} displayed a light intensity dependence with a slope of 1.92, 1.39, 0.93, and 1.12 kT q^{-1} for the device without and with the treatments of 1% NMP, 1% DPE, and the mixed additives, respectively. The device treated with mixed additives exhibited less charge-trapped recombination, which was consistent with the improved photovoltaic properties. These data also suggested that bimolecular recombination and space–charge effect were suppressed at J_{sc} conditions for the devices with the mixed solvent additives treatment.[57]

2.5. Morphology

To further gain insight into the effect of morphology of the photoactive layer for the PSCs, atomic force microscopy (AFM) and transmission electron microscopy (TEM) images were measured, as shown in **Figure 4**. The surface roughness and phase separation generated obvious changes for the PTZ1:PMI-F-PMI films with the treatments of solvent additives, indicating more enhanced or/and decreased aggregation of the donor and acceptor materials, due to the solubility difference of the donor or acceptor in the solvent additives. The surface roughness of the PTZ1:PMI-F-PMI blends without and with the treatments of 1% NMP, 1% DPE, and the mixed additives (0.5% NMP and 0.5% DPE) was 2.49, 5.51, 2.66, and 3.08 nm, respectively. The TEM images show similar tendency as that of the AFM images. Well-distributed nanofibrillar structures were observed in the TEM images, indicating enhanced phase separation, which are beneficial for increasing charge mobility. The results agree well with the increased FF of the devices with the treatment of the mixed additives.[54]

2.6. X-Ray Diffraction

To further throw light on the crystalline difference of pure donor and acceptor films and their blends without and with the treatment of solvent additives, X-ray diffraction patterns of the films spin-coated onto Si substrate were measured. As presented in **Figure 5**, the peaks at $2\theta = 4.58°$ and $2\theta = 5.10°$ for pure PTZ1 and PMI-F-PMI films are determined as (100) diffraction peaks, from which the interchain d-spacing of conjugated backbone was calculated to be 19.27 and 17.31 Å, respectively. The peak intensity of pure PMI-F-PMI film was weaker than that of PTZ1, indicating the interchain arrangement of donor was superior to that of acceptor. The diffraction intensity of PTZ1:PMI-F-PMI blend films with additive treatments showed a strong reflection at $2\theta = 4.45°$, compared with that of the blend without additive at $2\theta = 4.83°$, corresponding to an interchain d-spacing of 19.83 and 18.27 Å, respectively. The interchain arrangement and crystals of the blends with 1% NMP and 1% DPE were very similar; however, a strong interference of the blend at $2\theta = 4.45°$ was observed by using mixed additives (0.5% NMP + 0.5% DPE). The stronger XRD peak at $2\theta = 4.45°$ indicates the increased crystallinity (or ordered structure) of molecular backbone in the blend films with the mixed additive treatment in comparison to that of the blend without solvent additive treatment. The results confirm that the mixed additive treatment improved the aggregation morphology of the donor and acceptor materials, which agrees very well with the morphologies observed from the AFM and TEM images. Thus, these results implied that appropriate

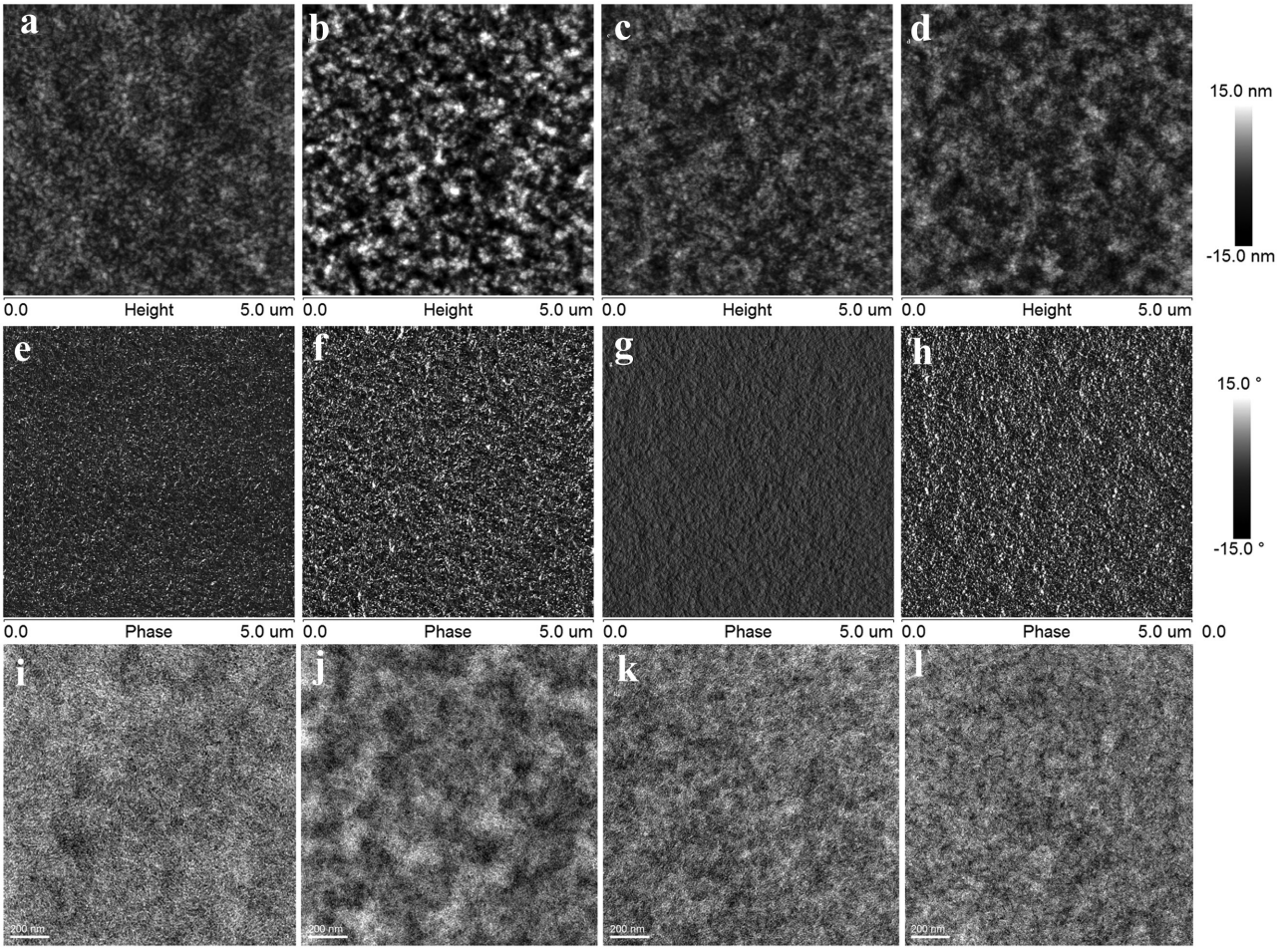

Figure 4. a–d) AFM height, e–h) phase, and i–l) TEM images of the PTZ1:PMI-F-PMI blend films (2:1, w/w) a,e,i) without and with the additive treatment of b,f,j) 1% NMP, c,g,k) 1% DPE, and d,h,l) 0.5% NMP + 0.5% DPE, respectively.

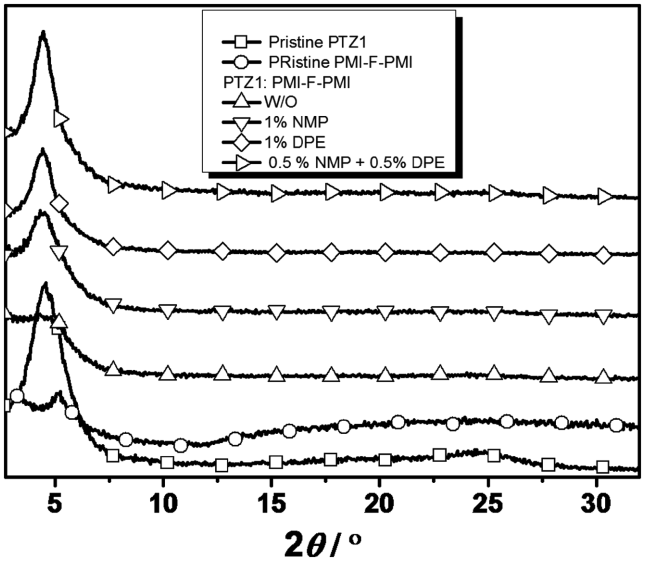

Figure 5. X-ray diffraction patterns of pristine PTZ1 and PMI-F-PMI films and the PTZ1:PMI-F-PMI blend film (2:1, w/w) without and with treatment of different solvent additives.

intermolecular aggregation promoted efficient charge transport and increased PCE of the PSCs.

3. Conclusion

In conclusion, we used a wide-bandgap conjugated polymer PTZ1 with deeper HOMO level as a donor and an n-OS PMI-F-PMI with higher LUMO level as an acceptor for the fabrication of high V_{oc} nonfullerene PSCs. The photovoltaic performance of the devices was optimized by changing donor/acceptor weight ratios and by the treatment of solvent additives. The PSCs based on PTZ1:PMI-F-PMI (2:1, w/w) with the treatment of mixed solvent additive of 0.5% NMP + 0.5% DPE showed a very high V_{oc} of 1.3 V with a good power conversion efficiency of 6.0% under the illumination of AM 1.5G, 100 mW cm^{-2}. The effect of the mixed solvent treatment on the photovoltaic performance was studied by the charge carrier mobility measurement and morphology analysis. The blend films with the mixed solvent treatment showed balanced hole and electron mobilities, smooth surface morphology, suitable phase separation, well-distributed nanofibrillar, and better crystalline structures, which are beneficial to the improvement of the

photovoltaic performance. The PCE of 6% is the highest for the PSCs with the high V_{oc} of 1.3 V. The results indicate that the active layer based on PTZ1/PMI-F-PMI could be used as a front layer in tandem PSCs for achieving high V_{oc} over 2 V, which will be beneficial for potential application in water splitting by photocatalysis.

Supporting Information

Supporting Information is available from the Wiley Online Library or from the author.

Acknowledgements

This work was supported by the National Natural Science Foundation of China (NSFC) (Grant Nos. 91333204, 51203168, 51422306, 51503135, and 51573120), the Priority Academic Program Development of Jiangsu Higher Education Institutions, Jiangsu Provincial Natural Science Foundation (Grant No. BK20150332), Natural Science Foundation of the Jiangsu Higher Education Institutions of China (Grant No. 15KJB430027), and the Ministry of Science and Technology of China (973 project, No. 2014CB643501).

Received: July 30, 2016
Revised: October 29, 2016
Published online:

[1] J. J. M. Halls, C. A. Walsh, N. C. Greenham, E. A. Marseglia, R. H. Friend, S. C. Moratti, A. B. Holmes, *Nature* **1995**, *376*, 498.
[2] G. Li, R. Zhu, Y. Yang, *Nat. Photonics* **2012**, *6*, 153.
[3] C. J. Brabec, N. S. Sariciftci, J. C. Hummelen, *Adv. Funct. Mater.* **2001**, *11*, 15.
[4] B. C. Thompson, J. M. J. Frechet, *Angew. Chem., Int. Ed.* **2008**, *47*, 58.
[5] J. Zhao, Y. Li, G. Yang, K. Jiang, H. Lin, H. Ade, W. Ma, H. Yan, *Nat. Energy* **2016**, *1*, 15027.
[6] M. C. Scharber, D. Mühlbacher, M. Koppe, P. Denk, C. Waldauf, A. J. Heeger, C. J. Brabec, *Adv. Mater.* **2006**, *18*, 789.
[7] P. W. M. Blom, V. D. Mihailetchi, L. J. A. Koster, D. E. Markov, *Adv. Mater.* **2007**, *19*, 1551.
[8] Y. He, H.-Y. Chen, J. Hou, Y. Li, *J. Am. Chem. Soc.* **2010**, *132*, 1377.
[9] X. Guo, C. Cui, M. Zhang, L. Huo, Y. Huang, J. Hou, Y. Li, *Energy Environ. Sci.* **2012**, *5*, 7943.
[10] Y. He, G. Zhao, B. Peng, Y. Li, *Adv. Funct. Mater.* **2010**, *20*, 3383.
[11] Y.-J. Cheng, C.-H. Hsieh, Y. He, C.-S. Hsu, Y. Li, *J. Am. Chem. Soc.* **2010**, *132*, 17381.
[12] X. Guo, M. Zhang, L. Huo, C. Cui, Y. Wu, J. Hou, Y. Li, *Macromolecules* **2012**, *45*, 6930.
[13] M. Svensson, F. Zhang, S. C. Veenstra, W. J. H. Verhees, J. C. Hummelen, J. M. Kroon, O. Inganäs, M. R. Andersson, *Adv. Mater.* **2003**, *15*, 988.
[14] C. E. Small, S. Chen, J. Subbiah, C. M. Amb, S.-W. Tsang, T.-H. Lai, J. R. Reynolds, F. So, *Nat. Photonics* **2012**, *6*, 115.
[15] Z. B. Henson, K. Müllen, G. C. Bazan, *Nat. Chem.* **2012**, *4*, 699.
[16] E. Wang, Z. Ma, Z. Zhang, K. Vandewal, P. Henriksson, O. Inganäs, F. Zhang, M. R. Andersson, *J. Am. Chem. Soc.* **2011**, *133*, 14244.
[17] M. Wang, X. Hu, P. Liu, W. Li, X. Gong, F. Huang, Y. Cao, *J. Am. Chem. Soc.* **2011**, *133*, 9638.
[18] J. Jo, A. Pron, P. Berrouard, W. L. Leong, J. D. Yuen, J. S. Moon, M. Leclerc, A. J. Heeger, *Adv. Energy Mater.* **2012**, *2*, 1397.
[19] L. Huo, J. Hou, S. Zhang, H. Y. Chen, Y. Yang, *Angew. Chem., Int. Ed.* **2010**, *49*, 1500.
[20] H.-Y. Chen, J. Hou, S. Zhang, Y. Liang, G. Yang, Y. Yang, L. Yu, Y. Wu, G. Li, *Nat. Photonics* **2009**, *3*, 649.
[21] Q. Peng, X. Liu, D. Su, G. Fu, J. Xu, L. Dai, *Adv. Mater.* **2011**, *23*, 4554.
[22] H. Zhou, L. Yang, A. C. Stuart, S. C. Price, S. Liu, W. You, *Angew. Chem., Int. Ed.* **2011**, *123*, 3051.
[23] M. Zhang, X. Guo, S. Zhang, J. Hou, *Adv. Mater.* **2014**, *26*, 1118.
[24] M. Zhang, Y. Gu, X. Guo, F. Liu, S. Zhang, L. Huo, T. P. Russell, J. Hou, *Adv. Mater.* **2013**, *25*, 4944.
[25] Z.-G. Zhang, Y. Li, *Sci. China: Chem.* **2015**, *58*, 192.
[26] J. Hou, M.-H. Park, S. Zhang, Y. Yao, L.-M. Chen, J.-H. Li, Y. Yang, *Macromolecules* **2008**, *41*, 6012.
[27] N. Blouin, A. Michaud, D. Gendron, S. Wakim, E. Blair, R. Neagu-Plesu, M. Belletete, G. Durocher, Y. Tao, M. Leclerc, *J. Am. Chem. Soc.* **2008**, *130*, 732.
[28] M. Zhang, X. Guo, X. Wang, H. Wang, Y. Li, *Chem. Mater.* **2011**, *23*, 4264.
[29] X. Guo, M. Zhang, J. Tan, S. Zhang, L. Huo, W. Hu, Y. Li, J. Hou, *Adv. Mater.* **2012**, *24*, 6536.
[30] Y. Liang, Z. Xu, J. Xia, S. T. Tsai, Y. Wu, G. Li, C. Ray, L. Yu, *Adv. Mater.* **2010**, *22*, E135.
[31] S. Alem, S. Wakim, J. Lu, G. Robertson, J. Ding, Y. Tao, *ACS Appl. Mater. Interfaces* **2012**, *4*, 2993.
[32] M. Neophytou, H. A. Ioannidou, T. A. Ioannou, C. L. Chochos, S. P. Economopoulos, P. A. Koutentis, G. Itskos, S. A. Choulis, *Polym. Chem.* **2012**, *3*, 2236.
[33] Z. Fei, M. Shahid, N. Yaacobi-Gross, S. Rossbauer, H. Zhong, S. E. Watkins, T. D. Anthopoulos, M. Heeney, *Chem. Commun.* **2012**, *48*, 11130.
[34] G. Zhao, Y. He, Y. Li, *Adv. Mater.* **2010**, *22*, 4355.
[35] S. Li, W. Liu, M. Shi, J. Mai, T.-K. Lau, J. Wan, X. Lu, C.-Z. Li, H. Chen, *Energy Environ. Sci.* **2016**, *9*, 604.
[36] Y. Fu, B. Wang, J. Qu, Y. Wu, W. Ma, Y. Geng, Y. Han, Z. Xie, *Adv. Funct. Mater.* **2016**, *26*, 5922.
[37] W. Yu, D. Yang, X. Zhu, X. Wang, G. Tu, D. Fan, J. Zhang, C. Li, *ACS Appl. Mater. Interfaces* **2014**, *6*, 2350.
[38] X. Zhang, J. Zhang, H. Lu, J. Wu, G. Li, C. Li, S. Li, Z. Bo, *J. Mater. Chem. C* **2015**, *3*, 6979.
[39] J. Zhang, X. Zhang, H. Xiao, G. Li, Y. Liu, C. Li, H. Huang, X. Chen, Z. Bo, *ACS Appl. Mater. Interfaces* **2016**, *8*, 5475.
[40] J. Zhang, X. Zhang, G. Li, H. Xiao, W. Li, S. Xie, C. Li, Z. Bo, *Chem. Commun.* **2016**, *52*, 469.
[41] J. Zhang, H. Xiao, X. Zhang, Y. Wu, G. Li, C. Li, X. Chen, W. Ma, Z. Bo, *J. Mater. Chem. C* **2016**, *4*, 5656.
[42] J. Zhao, Y. Li, H. Lin, Y. Liu, K. Jiang, C. Mu, T. Ma, J. Y. Lin Lai, H. Hu, D. Yu, H. Yan, *Energy Environ. Sci.* **2015**, *8*, 520.
[43] B. Guo, X. Guo, W. Li, X. Meng, W. Ma, M. Zhang, Y. Li, *J. Mater. Chem. A* **2016**, *4*, 13251.
[44] Y. Zhang, Y. Xiao, Y. Xie, L. Zhu, D. Shi, C. Cheng, *Org. Electron.* **2015**, *21*, 184.
[45] M. G. Walter, E. L. Warren, J. R. McKone, S. W. Boettcher, Q. Mi, E. A. Santori, N. S. Lewis, *Chem. Rev.* **2010**, *110*, 6446.
[46] W. Liu, S. Li, J. Huang, S. Yang, J. Chen, L. Zuo, M. Shi, X. Zhan, C. Z. Li, H. Chen, *Adv. Mater.* **2016**, *28*, 9729.
[47] J. Tong, S. Xiong, Y. Zhou, L. Mao, X. Min, Z. Li, F. Jiang, W. Meng, F. Qin, T. Liu, *Mater. Horiz.* **2016**, *3*, 452.
[48] J. Liu, S. Chen, D. Qian, B. Gautam, G. Yang, J. Zhao, J. Bergqvist, F. Zhang, W. Ma, H. Ade, O. Inganas, K. Gundogdu, F. Gao, H. Yan, *Nat. Energy* **2016**, *1*, 16089.
[49] C. Wang, X. Xu, W. Zhang, J. Bergqvist, Y. Xia, X. Meng, K. Bini, W. Ma, A. Yartsev, K. Vandewal, M. R. Andersson, O. Inganäs, M. Fahlman, E. Wang, *Adv. Energy Mater.* **2016**, *6*, 1600148.
[50] S. Holliday, R. S. Ashraf, C. B. Nielsen, M. Kirkus, J. A. Röhr, C.-H. Tan, E. Collado-Fregoso, A.-C. Knall, J. R. Durrant, J. Nelson, I. McCulloch, *J. Am. Chem. Soc.* **2015**, *137*, 898.

[51] S. Holliday, R. S. Ashraf, A. Wadsworth, D. Baran, S. A. Yousaf, C. B. Nielsen, C.-H. Tan, S. D. Dimitrov, Z. Shang, N. Gasparini, M. Alamoudi, F. Laquai, C. J. Brabec, A. Salleo, J. R. Durrant, I. McCulloch, *Nat. Commun.* **2016**, *7*, 11585.
[52] C. M. Proctor, M. Kuik, T.-Q. Nguyen, *Prog. Polym. Sci.* **2013**, *38*, 1941.
[53] Y. Liu, C. Mu, K. Jiang, J. Zhao, Y. Li, L. Zhang, Z. Li, J. Y. Lai, H. Hu, T. Ma, R. Hu, D. Yu, X. Huang, B. Z. Tang, H. Yan, *Adv. Mater.* **2015**, *27*, 1015.
[54] H. Zhong, C. H. Wu, C. Z. Li, J. Carpenter, C. C. Chueh, J. Y. Chen, H. Ade, A. K. Jen, *Adv. Mater.* **2016**, *28*, 951.
[55] S. R. Cowan, A. Roy, A. J. Heeger, *Phys. Rev. B* **2010**, *82*, 245207.
[56] O. K. Kwon, M. A. Uddin, J. H. Park, S. K. Park, T. L. Nguyen, H. Y. Woo, S. Y. Park, *Adv. Mater.* **2016**, *28*, 910.
[57] Y. Zhong, M. T. Trinh, R. Chen, G. E. Purdum, P. P. Khlyabich, M. Sezen, S. Oh, H. Zhu, B. Fowler, B. Zhang, W. Wang, C. Y. Nam, M. Y. Sfeir, C. T. Black, M. L. Steigerwald, Y. L. Loo, F. Ng, X. Y. Zhu, C. Nuckolls, *Nat. Commun.* **2015**, *6*, 8242.